

# Multiplexing and de-multiplexing of digital holograms recorded in microscopic configuration

Melania Paturzo<sup>\*a</sup>, Pasquale Memmolo<sup>a,b</sup>, Antonia Tulino<sup>b</sup>, Andrea Finizio<sup>a</sup>, Lisa Miccio<sup>a</sup>, and Pietro Ferraro<sup>a</sup>

<sup>a</sup>CNR - Istituto Nazionale di Ottica Applicata & Istituto di Cibernetica, via Campi Flegrei 34, 80078-Pozzuoli (NA), Italy

<sup>b</sup>DIET, Università di Napoli "Federico II", Via Claudio 21, 80125 Napoli, Italy

## ABSTRACT

We investigate the possibility to multiplexing and de-multiplexing numerically digital holograms recorded by means of a Mach-Zehnder interferometric microscope. The digital holograms are multiplexed and de-multiplexed thanks to the unique property of the digital holography to numerically manage the complex wavefields in different reconstruction planes. Two kind of multiplexing techniques are investigated. The first one allows to multiplex up to hundreds of digital holograms retrieving correctly quantitative information about their amplitude and phase maps. This technique can be used to optimize the storage of a large number of digital holograms or their transmission process from a recording head to a remote display unit. The second method consists in the angular multiplexing and de-multiplexing of several digital holograms. This technique has been performed rotating numerically one hologram at different angles and adding all the rotated holograms to obtain a single synthetic digital hologram. However, for this technique, a multiplexed digital hologram can be also obtained rotating the CCD array during the holograms recording process. The distortions caused by the multiplexing/de-multiplexing procedures has been evaluated for both the techniques.

**Keywords:** Digital holography, microscopy, Fourier optics and signal processing.

## 1. INTRODUCTION

Digital Holograms can be multiplexed by encoding the information of two or more holograms in a single one. Multiplexing of digital holograms has been used to measure some object properties, as the state of polarization, dynamical phenomena or three-dimensional mechanical deformations by a single image acquisition [1,2]. For example in [2] a multiplexing and de-multiplexing technique for digital holograms is developed in order to obtain the simultaneous determination of the in-plane and the out-of-plane components of the displacement vector of an object submitted to mechanical loading. Other applications of multiplexing techniques in holography regard the investigation of ultra-fast events. Holographic recording of nanosecond events on a conventional CCD camera is achieved acquiring multiple pulsed holograms on a single CCD frame, at the same time [3]. A measurement of the full spatio-temporal electric field of a femtosecond laser pulse on a single shot is obtained by wavelength multiplexed DH. The recorded digital hologram contains multiple spectrally resolved smaller holograms, each of one characterizes the spatial intensity and phase distributions of an individual frequency component of the pulse [4]. Moreover, spatial multiplexing is exploited in DH experiments in which a diffraction grating is introduced into the set-up to get super-resolved images increasing synthetically the numerical aperture of the image sensor [5,6].

Actually, in the most of the above mentioned approaches, spatial multiplexing of digital holograms is obtained optically, that means recording simultaneously more than one fringe pattern on the same sensor array. Depending on the different experiments, one or more reference beams with different angles are used to obtain interference fringe patterns with different spatial frequencies and oriented along different directions. All the holograms are superimposed in one composite CCD frame, and each of them can be independently reconstructed after the digital spatial filtering in the Fourier spectral domain of the multiplexed hologram.

However, the multiplexing operation can be carried out also by numerical techniques by combining numerically digital holograms to obtain a single synthetic hologram. Recently, we demonstrated that an efficient storage and/or transmission

of a large number of digital holograms can be attained by numerical multiplexing (NM) method [7]. The results obtained are reported in the section 3.

On the other hand, we studied also a different approach to encode information from various digital holograms acquired in microscope configuration in a multiplexed one, through the angular rotation of the digital holograms around their optical axis. This method can be implemented numerically or optically. In the first case, each hologram is rotated numerically. Then, the combination is performed by the simple summation of the numerically rotated digital holograms. In the second case, the multiplexing can be obtained through the rotation of the object as well as of the detector (i.e. CCD array) around its centre in the x-y plane, that is in a plane parallel to the hologram plane. In the section 4, we present the results obtained in the first case.

## 2. EXPERIMENTAL SET-UP

In both the mentioned approach, reported in the following sections, we exploit the unique capability of DH to manage numerically the complex wavefronts, to reconstruct the object wave field at an intermediate plane, that is, essentially, the back focal plane (BFP) of the imaging lens. In fact, the multiplexed holograms are acquired by means of a Mach-Zehnder interferometric microscope, shown in Fig.1. The laser wavelength is 532 nm and the microscope objective is a 20 X objective with a focal length  $f=9.0$  mm and a NA=0.40. The CCD detector has 1280 X 1024 square pixel which size  $P_{CCD} = 6.7 \mu\text{m}$ .

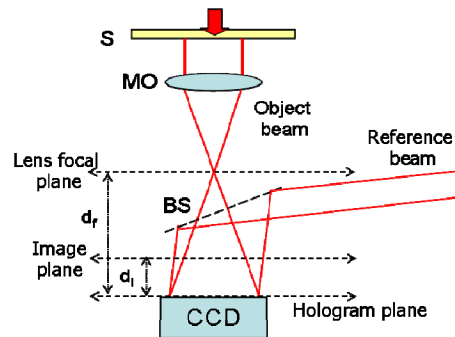


Fig. 1. Sketch of the DH setup; S: sample; BS: beam splitter; MO: microscope objectives.

In the BFP of the imaging lens, the complex-value array, corresponding to the object wavefield, is proportional to the Fourier transform of the complex amplitude of the wave at an input plane, regardless of its distance  $d$  from the lens, according to the following equation [8],

$$g(x, y) = h_l h_d F\left(\frac{x}{\lambda f}, \frac{y}{\lambda f}\right) \quad (1)$$

where  $h_d = \exp [i\pi (x^2 + y^2)(d-f) / \lambda f^2]$  is a phase factor depending on  $d$  while  $h_l = (i / \lambda f) \exp(-i4\pi f / \lambda)$ ,  $f$  is the focal length and  $\lambda$  is the laser wavelength. Therefore, we obtain only the spectrum of the object wave field, removing the contribution of the carrier frequencies (that is the chirped phase factor coming from the interference between the plane reference beam and the curvature of the object beam introduced by the microscope objective).

### 3. ALL NUMERICAL MULTIPLEXING/DEMULPLEXING

In this section we described the first method we use for the numerical multiplexing and de-multiplexing of up to 100 digital holograms. This technique could be useful to optimize the transmission of digital holograms from the recording head and the display unit being in separate locations [9,10]. Firstly, we will show how the holograms are multiplexed and, then, how the multiplexed hologram is processed in order to reconstruct all one hundred amplitude and phase maps. Finally, these reconstructed images are compared with those one obtained by the original holograms and the distortions caused by the multiplexing are evaluated.

The specimen is an in vitro mouse preadipocyte 3T3-F442A cell. It has been monitored for 25 hours to investigate its activities and one hundred holograms have been recorded with an acquisition rate of 4frame/ hour. Moreover, a reference hologram is acquired in a area of the sample far from the cell, that is in the culture medium, in order to calculate the phase retardation caused only by the cell presence in the optical path subtracting the phase shift due to the interferometer and the culture medium. Each of the hologram is reconstructed in the back focal plane of the MO. The amplitude reconstruction of one hologram in the BFP, at the distance  $d_f=400$  mm from the hologram plane, is shown in Fig.2(a).

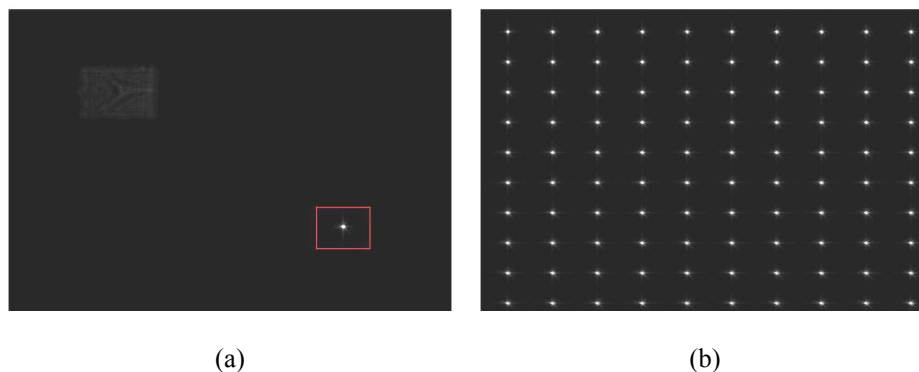


Fig. 2: (a) Amplitude reconstruction of one hologram in the back focal plane (BFP). The red frame indicates the used filtering window, 50 X 50 square pixels around the carrier frequency of the object spectrum. (b) Amplitude of the synthetic spectrum obtained by the numerical multiplexing in the BFP of 100 digital holograms.

Then, we choose a mask to filter each hologram in the BFP. The red frame in Fig.2(a) indicates the shape and the dimension of the used filtering window, that is 50 X 50 pixels around the carrier frequency of the object spectrum, whose position depends on some geometrical parameters of the experimental setup such as the angle between the reference and the object beams and on the reconstruction distance  $d$ . The transmittance of the mask is 1 within the frame and 0 outside. Obviously, reducing the dimension of the filtering window will increase the number of holograms we can encode in one single hologram. On the other hand, the size of the filtering window should be larger than the object bandwidth in order to retain the spectral information.

In our case, the chosen mask allows to simply multiplex all 100 holograms. To properly multiplex the holograms in the BFP, we join together the filtered spectra shifting the carrier frequency of each hologram  $h_{m,n}$  by a value  $\vec{s} = (m\vec{x} + n\vec{y})p$  where  $m$  and  $n$  are integer numbers ranging from 1 to 10 whereas  $p$  is the size of the filtering window. The amplitude of the synthetic spectrum obtained in this way is shown in Fig.2(b). The hologram  $h_{1,1}$  corresponds to the reference hologram. This complex-value array contains the information about the phase and amplitude of all one hundred holograms. It has to be transmitted with the multiplexing key. In fact, the numerical de-multiplexing needs the precise knowledge of the frequencies of the spatial carrier waves of all the holograms. Therefore, the receiver can de-multiplexed the synthetic spectrum and reconstruct all one hundred holograms only knowing the multiplexing key that have to be send together with the synthetic spectrum.

In the de-multiplexing process, the hologram composed in the BFP is filtered selecting one by one the single holograms that, then, are numerically reconstructed in the image plane.

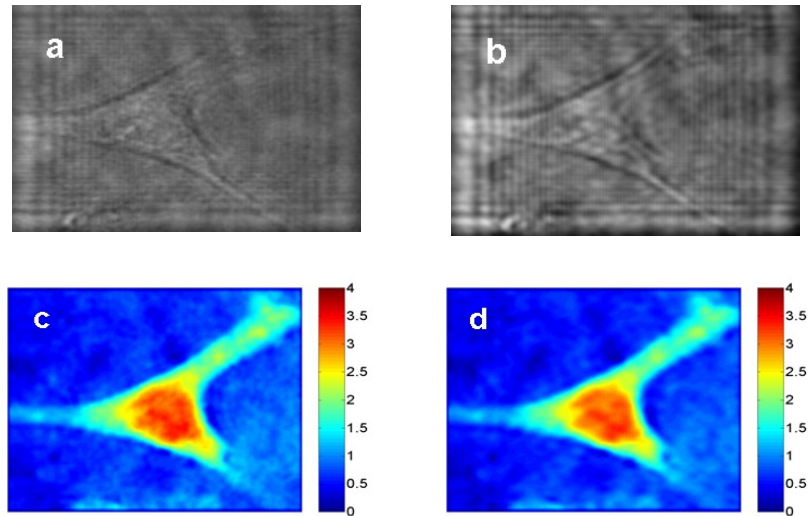


Fig. 3: Amplitude and phase reconstructions of one hologram as acquired by the CCD (a, c) and after the multiplexing/de-multiplexing process (b, d).

In Fig. 3 are shown the amplitude and phase reconstructions of one hologram as acquired by the CCD (left) and after the multiplexing/de-multiplexing process (right). Comparing the two kind of reconstructions, the distortion caused by the filtering process is not evident. In Fig.4 we have plotted the difference between the two phase reconstructions in order to evaluate the distortion. Then, we calculated the mean value and the variance of the two-dimensional distribution of this phase difference. The mean value is 0.068 rad with a variance of  $1 \cdot 10^{-3}$  rad, while the maximum value is 0.23 rad. Looking at Fig. 4, it is clear that the maximum phase difference is situated on the cell border. This result is caused by the use of the filtering window that acts as a band-pass filter with limited bandwidth, cutting the high spatial frequencies due to the edges.

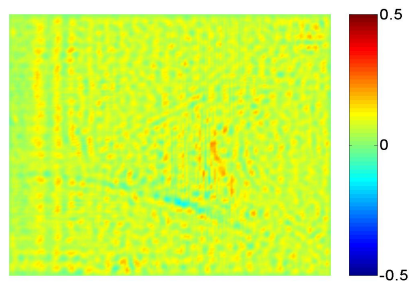


Fig. 4: Single frame excerpts from the movie of the 2D distribution of the difference between the two phase reconstructions in Fig. 3(c) and 3(d).

#### 4. ANGULAR MULTIPLEXING/DEMULPLEXING

In this section we present a different approach to encode information from various digital holograms acquired in microscope configuration in a multiplexed one, through the angular rotation of the digital holograms around their optical axis. By the proposed method we multiplex numerically up to five digital holograms. Then we create its five rotated replicas turning it around its centre by a fixed angle  $\alpha=30^\circ$ . The specimen used is a particular type of MEMS (micro-electromechanical system).

Each hologram is padded with zeros [11] up to 1400 X 1400 square pixels to allow the whole five rotated holograms to be contained in the multiplexed hologram. Obviously the dimension of the padding window depends on the chosen angle of rotation. Then we add the five holograms in order to multiplexed them in a single synthetic hologram shown in Fig. 5.

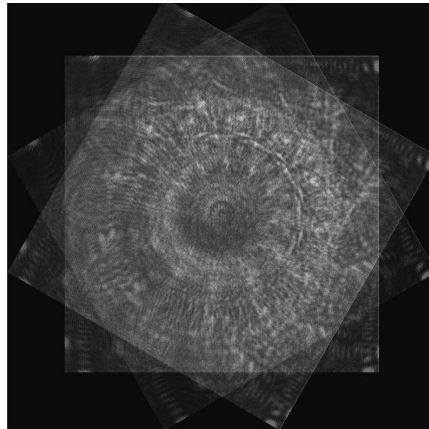


Fig. 5. Multiplexed synthetic hologram obtained adding five rotated holograms.

Moreover, a reference hologram is acquired in a region of the sample far from the MEMS in order to calculate the phase retardation caused only by the MEMS subtracting the phase shift due to the interferometer. The reference hologram is multiplexed in the same way of the MEMS hologram. The multiplexing of the reference hologram is needed to avoid distortion effects in the reconstructed phase maps. In fact, the rotation of the hologram is obtained through a cubic interpolation algorithm that introduces some distorting effects. In order to avoid that these distortions affect the retrieved phase map, both the MEMS holograms and references holograms have to be processed in the same way. Therefore the two holograms experience the same distortion that is eliminated when the phase map is retrieved by calculating the difference between the two holograms.

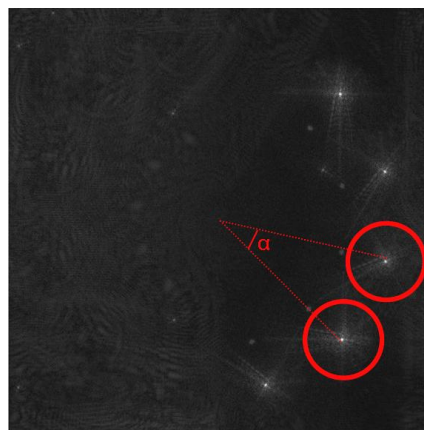


Fig. 6. Amplitude reconstruction of the multiplexed hologram in the BFP. The red frames indicate the circular filtering windows used to de-multiplex the holograms.

The reconstruction of the multiplexed hologram in the BFP of the imaging lens, shown in Fig. 6, corresponds to the spectrum of the object wave, centred around a carrier frequency that depends on some geometrical parameters of the experimental setup. Then, we choose a mask to filter each hologram in the BFP. The red frame in Fig. 6 indicates the shape and the dimension of the used filtering window, that is a circular window with a radius of 100 pixels, centred around the carrier frequency of the object spectrum. The transmittance of the mask is 1 within the frame and 0 outside. To extract all the five holograms, we rotate the mask with step of  $\alpha$ , maintaining as pivot the centre of the reconstruction plane (as shown in Fig. 6). Then, each single wavefield is filtered and numerically back-propagated in the hologram plane. Then, the complex wavefields are rotated in the hologram plane by steps of  $-\alpha$  by means of the same interpolation routine used in the multiplexing process. Finally these filtered holograms are reconstructed in the image plane. Fig. 7 shows the amplitude reconstruction for the hologram rotated by  $\alpha=30^\circ$ . Several replicas of the reconstructed image appear. They are caused by the interpolation routine used to rotate the filtered holograms.

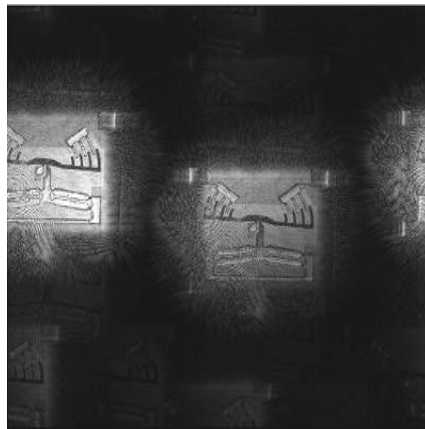


Fig. 7. Amplitude reconstruction for one filtered hologram in the image plane. Several replicas of the reconstructed image appear.

To filter out this replicas, the complex wavefield is propagated again in the lens BFP where their overlapping is minimum (see Fig. 8). Then, the same mask employed in the de-multiplexing process is applied to filter the replicas in the complex wavefield that then is propagated back to the hologram plane and finally in the image plane. In this way we minimized the distortion caused by the interpolation routine.

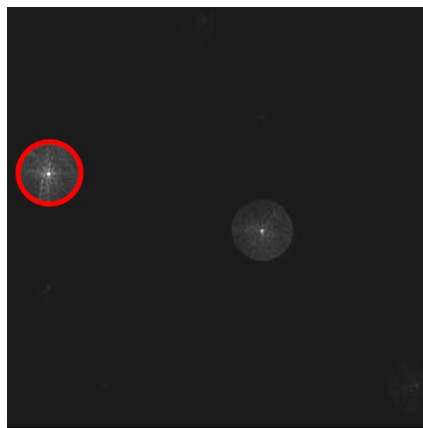


Fig. 8. Amplitude reconstruction for one filtered hologram in the BFP. The same mask employed in the de-multiplexing process is applied to filter the replicas.

The complex wavefield is propagated back to the hologram plane and then in the image plane to make the pixel of reconstruction in the image plane independent from the distance between the BFP and the image plane [12]. The final amplitude and phase reconstructions are shown in Figs. 9(a) and 9(b) for the hologram rotated by  $\alpha=30^\circ$ . To obtain the phase reconstruction, the phase of the reference hologram rotated by the same angle has been subtracted.

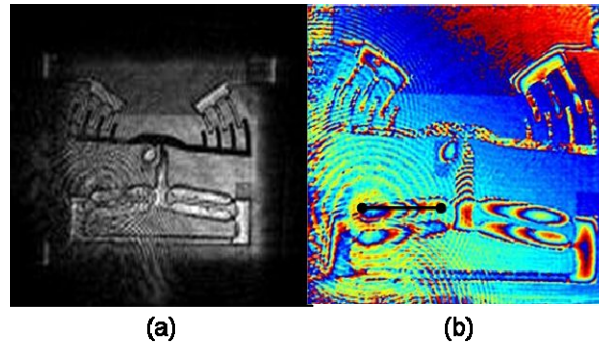


Fig. 9. Final amplitude and phase reconstructions of one filtered hologram after the de-multiplexing process by rotation in the hologram plane.

We can compare the reconstructions obtained by the proposed technique to those one coming from the original hologram, showed in Fig. 10. The noise present in the reconstructions of the de-multiplexed hologram (see Fig. 9) is caused by the overlapping of the objects spectra (see Fig. 6). Obviously, the smaller angle  $\alpha$  is, that is the higher the number of multiplexed holograms is, the larger is the overlapping area between two close reconstructions in the BFP. Moreover, for a fixed  $\alpha$ , to decrease the effects of the overlapping we can diminish the radius of filtering window, but, in this case, also the spectral information of the filtered hologram and, therefore, the quality of the final reconstructed image are reduced. Therefore, according to the shape of the holograms spectra, we have to find the right arrangement between the number of multiplexed holograms and the acceptable noise in the amplitude and phase reconstructions.

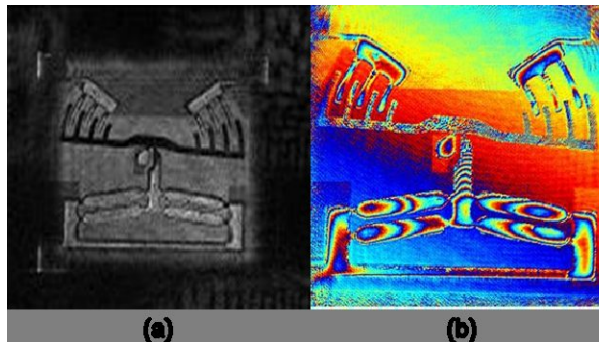


Fig. 10. Amplitude and phase reconstructions of one hologram as acquired by the CCD.

## 5. CONCLUSION

In conclusion, we proposed two techniques for the multiplexing and de-multiplexing of digital holograms acquired in microscope configuration. The first method is an all numerical multiplexing/de-multiplexing technique. We demonstrated that up to 100 DHs can be multiplexed and de-multiplexed correctly using this method. The phase distortions caused by this procedure has been evaluated and results on average less than 0.07 rad. This technique could be useful to perform an efficient storage and/or a fast transmission of DHs from the recording head to the display unit. The second method we studied is an angular multiplexing/de-multiplexing technique that allows to multiplex five holograms and to retrieve correctly quantitative information about the amplitude and phase maps through the numerical de-multiplexing. The results coming from this investigation could be helpful in some super-resolution techniques where the object is rotated to collect the most possible of the spatial frequencies of its diffraction spectrum by a CCD array [13,14].

## REFERENCES

- [1] Colomb, T., Dürr, F., Cuche, E., Marquet, P., Limberger, H. G., Salathé, R.-P. and Depeursinge, C., "Polarization microscopy by use of digital holography: application to optical-fiber birefringence measurements," *Appl. Opt.* 44, 4461-4469 (2005).
- [2] Picart, P., Moisson, E. and Mounier, D., "Twin-Sensitivity Measurement by Spatial Multiplexing of Digitally Recorded Holograms," *Appl. Opt.* 42, 1947-1957 (2003).
- [3] Liu, Z., Centurion, M., Panotopoulos, G., Hong, J. and Psaltis, D., "Holographic recording of fast events on a CCD camera," *Opt. Lett.* 27, 22-24 (2002).
- [4] Gabolde, P. and Trebino, R., "Single-shot measurement of the full spatio-temporal field of ultrashort pulses with multi-spectral digital holography," *Opt. Express* 14, 11460-11467 (2006).
- [5] Liu, C., Liu, Z., Bo, F., Wang, Y. and Zhu, J., "Super-resolution digital holographic imaging method," *Appl. Phys. Lett.* 81, 3143 (2002).
- [6] Paturzo, M., Merola, F., Grilli, S., De Nicola, S., Finizio, A. and Ferraro, P., "Enhanced super-resolution in digital holography by a dynamic phase grating," *Opt. Express* 16, 17107-17118 (2008).
- [7] Paturzo, M., Memmolo, P., Miccio, L., Finizio, A., Ferraro, P., Tulino, A. and Javidi, B., "Numerical multiplexing and demultiplexing of digital holographic information for remote reconstruction in amplitude and phase," *Opt. Lett.* 33, 2629-2631 (2008).
- [8] Saleh, B.E.A. and Teich, M. C., [Fundamentals of Photonics], Wiley-Interscience Publication, John Wiley and Sons, Inc. (1991).
- [9] Zegers, I., Carotenuto, L., Evrard, C., "Counterdiffusion protein crystallisation in microgravity and its observation with PromISS (Protein Microscope for the International Space Station)" *Microgravity sci. technol.* XVIII-3/4, 165-169 (2006).
- [10] Watson, J., Alexander, S., Craig, G., "Simultaneous in-line and off-axis subsea holographic recording of plankton and other marine particles," *Meas. Sci. Technol.* 12, L9-L15 (2001).
- [11] Ferraro, P., De Nicola, S., Coppola, G., Finizio, A., Alfieri, D. and Pierattini, G., "Controlling image size as a function of distance and wavelength in Fresnel-transform reconstruction of digital holograms," *Opt. Lett.* 29, 854-856 (2004).
- [12] Zhang, F. and Yamaguchi, I., Yaroslavsky, L. P., "Algorithm for reconstruction of digital holograms with adjustable magnification," *Opt. Lett.* 29, 1668-1670 (2004).
- [13] Alexandrov, S. A., Hillman, T. R., Gutzler, T. and Sampson, D. D., "Synthetic Aperture Fourier Holographic Optical Microscopy," *Phys. Rev. Lett.* 97, 168102 (2006).
- [14] Kuznetsova, Y., Neumann, A. and Brueck, S. R., "Imaging interferometric microscopy—approaching the linear systems limits of optical resolution," *Opt. Express* 15, 6651-6663 (2007).